By low-loss SEM, the head (*h*) of the 3C phage appears cylindrical (Figs. 2 and 3). Two slightly different head configurations are observed in SEM, STEM, and TEM micrographs. Most of the phage heads have straight, parallel sides along the vertical (long) axis. Other heads appear swollen; the length of the head remains constant, but the sides of the long axis appear to bulge, or seem dented or collapsed (Fig. 2, arrow). By STEM we find that these bulging or collapsed heads are more transparent, suggesting that they are devoid of nucleic acid. The altered head morphology may be due to capsid fragility after nucleic acid expulsion. When compared to the size of phage heads seen by STEM, those observed by SEM appear uniformly larger. We attribute this fact to the metal coating on the surface of the SEM sample (approximately 50 Å in thickness).

At the point of attachment of the head, the tail (*t*) narrows markedly (*n*), appearing one-half as thick (Figs. 1 to 3). This is similar to the TEM micrographs of Tikhonenko (*9*), who reported a narrowing of the tail in the neck region (*n*) of negatively stained phage Polonus X of *Mycobacterium tuberculosis*, a similar noncontractile phage. When examined at high magnifications, the end plate of the tail is found to consist of a number of lobular projections (Fig. 4), which corresponds to the postulated type III end plate found in group IV phages (*10*). To our knowledge this is the first time this structure has been verified.

Low-loss SEM images of the T4 coliphage clearly show the head, tail, and end plate (*11*) (Figs. 5 to 7). At the junction between the head and tail, there appears to be a band girdling the neck, corresponding to the "tail collar" first reported by Anderson (*12*) (Figs. 5 and 6, white arrows). In some instances, it seems possible in the SEM image to resolve the period of the helical tail sheath (Fig. 6, white arrow). At the base of the tail there is an enlarged region, and at high magnifications small projections (*s*) can be seen extending from the end plate (Figs. 5 to 7). In cases where the tail is uppermost, the sixfold symmetry of the end plate is clearly seen together with the central core (Fig. 7, black line). STEM images of coliphages show similar spikes projecting from the lower surface of the end plate (*13*). Also in the untriggered phage, long, thin, threadlike structures extend from the end plate up along the vertical axis of the tail and often project onto the head (Fig. 5, black arrows). These may be the tail fibers that were not obscured by the metal coating. We also find the tail fibers in this position in STEM micrographs.

Small globular particulates are observed on the surfaces of both bacteria and phages (particulate size, 10 to 30 Å) at very high magnifications (Figs. 5 to 7). These particulates are presumed to be a product of the coating rather than significant biological ultrastructure, because they are also seen on the otherwise smooth surface of the SiO_2 substrate. We have found that the amount of ultrastructural detail that is obscured by the coating is significantly less when the coating thickness is reduced. For example, see Fig. 6 where there is clear evidence of the period of the helical sheath (arrow), whereas in Fig. 5 this periodicity is obscured. The coating in Fig. 6 was 25 Å compared to 50 Å in Fig. 5. It should be possible by refinement of the evaporation technique to further reduce the granularity of the evaporated coating. It may also be that sufficient density can be provided to the specimen by surface doping with material of high atomic number through the use of a binding agent (*14*). Preliminary experiments in which heavy metal staining procedures have been used to enhance contrast have proven successful (*15*).

We have successfully shown that surface and internal ultrastructure of phages can be studied at useful magnifications as high as 500,000× and point-to-point resolution approaching 20 Å (7-Å resolution using the "width of the dark space" criterion) by SEM using the low-loss method (*2*), and by STEM operation of the same instrument at resolution similar to TEM. The clarity of the micrographs, superior resolution, lack of sample charging effects, and versatility of examination of SEM and STEM make this a superior tool for biological ultrastructural research. The technology used in the microscope is quite similar to that used in today's commercial electron microscopes. The limiting factor in high-resolution SEM is not only the instrument, but equally the specimen preparation, and as with most advances in microscopy, improved methods of specimen preparation are just as important as improvements to the microscope itself.

A. N. BROERS
IBM Thomas J. Watson Research Center, Yorktown Heights, New York 10598

B. J. PANESSA
J. F. GENNARO, JR.
St. Vincent's Hospital and *Laboratory of Cellular Biology, New York University, New York 10003*

References and Notes

1. A. N. Broers, *Appl. Phys. Lett.* **22**, 610 (1973).
2. A. V. Crewe and J. Wall, *J. Mol. Biol.* **48**, 375 (1970).
3. O. C. Wells, A. N. Broers, C. G. Bremer, *Appl. Phys. Lett.* **23**, 353 (1973).
4. Lens aberration data obtained from data of M. B. Heritage, IBM Thomas J. Watson Research Center, Yorktown Heights, New York.
5. O. C. Wells, *Appl. Phys. Lett.* **19**, 232 (1971).
6. I. Kondo and N. Hasegawa, *JEOL (Jpn. Electron. Opt. Lab.) News* **12**, 16 (1974).
7. B. J. Panessa and J. F. Gennaro, Jr., in *IITRI Scanning Electron Microscopy/72*, O. Johari, Ed. (IITRI, Chicago, 1972), p. 327.
8. T. F. Anderson, *Trans. N.Y. Acad. Sci.* **13**, 130 (1951).
9. D. Bradley, *J. Ultrastruct. Res.* **8**, 552 (1963).
10. A. Tikhonenko, *Ultrastructure of Bacterial Viruses* (Plenum, New York, 1970).
11. M. Moody, *Virology* **26**, S67 (1965).
12. T. F. Anderson, in *Proceedings of the European Regional Conference on Electron Microscopy, Delft, 1960* (Nederlandse Vereniging voor Electronen Microscopie, Delft, 1960), vol. 2, p. 1008.
13. W. Wood and R. Edgar, in *Molecular Basis of Life*, R. Haynes and P. Hanawolt, Eds. (Freeman, San Francisco, 1968), p. 153.
14. R. O. Kelley, R. A. F. Dekker, J. G. Bluemmk, *J. Ultrastruct. Res.* **45**, 254 (1973).
15. A. N. Broers, B. J. Panessa, J. F. Gennaro, Jr., in *IITRI Scanning Electron Microscopy/75*, O. Johari, Ed. (IITRI, Chicago, 1975), p. 233.
16. We thank the Phage Typing Laboratory and Dr. Oishi of the New York Department of Public Health, and Bill Rosenzweig and Milton Schiffenbauer of New York University, Washington Square, for their assistance in growing the phages. John Sokolowski is also recognized for designing and building many of the critical components of the new SEM.

11 March 1975; revised 15 April 1975

Distribution of Concanavalin A Receptor Sites on Specific Populations of Embryonic Cells

Abstract. *The early 32- to 64-cell stage of the sea urchin embryo consists of three cell types, easily distinguishable by size: micromeres, mesomeres, and macromeres. Only the micromeres are migratory. Treatment of dissociated sea urchin embryo cells with fluorescein-labeled concanavalin A (Con A) revealed a Con A–induced highly clustered or capped distribution of receptor sites on the micromeres. Concanavalin A did not induce significant clustering or capping of receptor sites on the mesomeres or macromeres. The results indicate that Con A receptor sites are more mobile on specific populations of malignant-like migratory embryonic cells.*

Plant lectins, which bind to specific cell surface carbohydrate residues, have been used in recent years to explore many aspects of the structure and function of cell surfaces. One such lectin, concanavalin A (Con A) causes agglutination of transformed cells and embryonic cells, but not their normal or adult counterparts without previous trypsinization (*1*). Concanavalin A is capable of binding to nonagglutinable cell types. However, it seems to induce a clustering of Con A binding sites only in the membranes of cell types that are agglutinable (*2, 3*).

It has been proposed that during morphogenesis the orderly shifts of individual

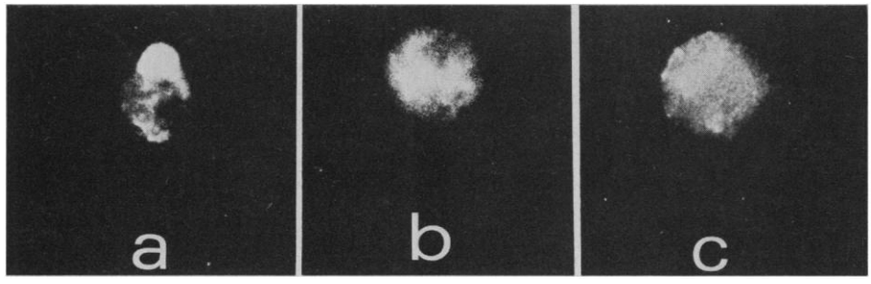

Fig 1. Concanavalin A receptor site distribution on the surface of a micromere, mesomere, and a macromere. Gametes of the sea urchin *Strongylcentrotus purpuratus* were obtained by injection of 0.55*M* KCl. The egg suspensions were treated and fertilized as described (*8*). The zygotes were distributed into beakers and allowed to develop at 17°C until the 32- to 64-cell stage was reached. Zygotes were collected and washed three times in CMF-SW with 1 percent Ficoll. Each 3 ml of packed cells was incubated for 10 minutes in 2 ml of 0.01*M* EGTA [ethylene-bis-(oxyethylenenitrilo)tetraacetate] in CMF-SW with 1 percent Ficoll and gently aspirated to complete dissociation. This cell suspension was diluted with 10 ml of CMF-SW with 1 percent Ficoll and layered over a 5 to 15 percent Ficoll discontinuous gradient made in a beaker. The beaker was placed in a 17°C incubator for 3 hours in order to separate out any cell debris, unfertilized eggs, or undissociated embryos. Cells were removed from the gradient, washed twice, and treated with FITC–Con A (750 μg/ml; Miles-Yeda) for 10 minutes in a rotating suspension at 17°C and washed in CMF-SW with 1 percent Ficoll. The cells were then fixed with 4 percent formaldehyde in CMF-SW with 1 percent Ficoll for 20 minutes, washed twice, and mounted on slides. (a) Micromere; (b) mesomere; (c) macromere. The experiment was repeated four times with different batches of cells. In all cases 95 percent of the micromeres appeared capped or highly clustered under the above conditions, while the mesomeres and macromeres displayed random site distributions.

cells and cell complexes may be due to differential cell surface properties (*4*). These morphogenetic movements, especially during gastrulation, of migratory embryonic cells represent a behavior pattern that is similar to invasiveness characteristic of malignant cells. Moscona has suggested that the Con A receptor sites may be associated with the capacity of malignant and embryonic cells to migrate and infiltrate (*5*). Dissociated sea urchin embryo cells and chick embryo cells are more agglutinable with Con A at early stages of development than at later stages (*6*). The decrease in Con A agglutinability occurs at a time when there is also a decrease in migratory activity.

By the use of a quantitative agglutination assay (*7*) we have shown that the micromere is the only cell type at the 32- to 64-cell stage of the sea urchin embryo that is agglutinable with Con A (*8*). Macromeres and mesomeres, the other cell types present, are not significantly agglutinable with Con A (*8*).

We now report a striking difference between the visual display patterns of the Con A receptor sites of the micromere and those of the nonmigratory embryonic cell types (macromeres and mesomeres).

Embryos were prepared and dissociated as described (*8*). The dissociated sea urchin embryo cells were fixed for 20 minutes in 4 percent formaldehyde in calcium-magnesium-free seawater (CMF-SW) with 1 percent Ficoll. Fluorescein isothiocyanate conjugated Con A (FITC–Con A, Miles-Yeda) was added to cell suspensions at a concentration of 750 μg/ml. Suspensions were rotated for 10 minutes at 17°C and washed twice in CMF-SW with 1 percent Ficoll before mounting on slides. When these cells were examined under the Leitz Orthoplan phase contrast fluorescence microscope (with incident illumination from a xenon lamp) the distribution of Con A receptor sites appeared to be random on all three embryonic cell populations. However, if the cells were treated with FITC–Con A before fixation the receptor sites on the micromeres were capped or highly clustered on about 95 percent of the cells (Fig. 1). The distribution of Con A receptor sites on the mesomeres and macromeres remained random under these procedures (Fig. 1). The fluorescence observed did not appear to be due to the uptake of FITC–Con A by the cells because at least 95 percent of the fluorescence was removed by incubating the FITC–Con A treated cells in 0.4*M* α-methyl-D-glucoside solution for 20 minutes. No fluorescence was visible to the eye, in the latter experiment.

The Con A–induced clustering and capping of the receptor sites on the micromeres indicates that the lateral mobility of these sites is similar to that observed in malignant cell types (*2*, *3*). The greater lateral mobility of the Con A receptor sites on migratory cell types such as embryonic cells, lymphocytes, and neoplastic cells may be due to (i) a greater intrinsic fluidity of the lipid bilayer; (ii) a structural modification of the Con A receptor sites; or (iii) alterations in the structure of microtubules and microfilaments attached to the inner membrane surface, which might effect the mobility of membrane proteins and glycoproteins. These possibilities and others have been discussed by Nicolson (*3*).

MARIE ROBERSON
ANTHONY NERI
STEVEN B. OPPENHEIMER
Department of Biology, California State University, Northridge 91324

References and Notes

1. N. Sharon and H. Lis, *Science* **177**, 949 (1972).
2. G. L. Nicholson, *Nat. New Biol.* **239**, 193 (1972); *ibid.* **243**, 218 (1973); M. Inbar and L. Sachs, *FEBS (Fed. Eur. Biochem. Soc.) Lett.* **32**, 124 (1973); J. Z. Rosenblith, T. E. Ukena, H. H. Yin, R. D. Berlin, M. J. Karnovsky, *Proc. Natl. Acad. Sci. U.S.A.* **70**, 1625 (1973).
3. G. L. Nicolson, *Int. Rev. Cytol.* **39**, 89 (1974).
4. P. L. Townes and J. Holtfreter, *J. Exp. Zool.* **128**, 53 (1955).
5. A. A. Moscona, *Science* **171**, 905 (1971).
6. S. W. Krach, A. Green, G. L. Nicolson, S. B. Oppenheimer, *Exp. Cell Res.* **84**, 191 (1974); S. J. Kleinschuster and A. A. Moscona, *ibid.* **70**, 297 (1972).
7. S. B. Oppenheimer and J. Odencrantz, *ibid.* **73**, 475 (1972).
8. M. M. Roberson and S. B. Oppenheimer, *ibid*, **91**, 263 (1975).
9. We thank D. L. Morton and W. D. Winters for the use of facilities and the fluorescence microscope. This research was supported by PHS research grant CA 12920 (S.B.O.).
* Address reprint requests to S.B.O.

17 March 1975; revised 23 April 1975

Juvenile Hormone Analogs: Detrimental Effects on the Development of an Endoparasitoid

Abstract. *A high incidence of mortality of the endoparasitoid* Aphidius nigripes *was observed when its host,* Macrosiphum euphorbiae, *was treated with juvenile hormone analogs. Larval and pupal stages of the parasitoid were susceptible. Off-target effects on natural enemies may seriously limit the use of juvenile hormone analogs, especially in integrated control programs.*

The potential of juvenile hormone analogs, the so-called "third generation" insecticides, as a means of controlling insect pests has been well documented. Observed effects include increased mortality (*1*), reduced fecundity (*2*), altered mating behavior (*3*), inhibition of dispersal due to abnormal wing development (*4*), and termination of diapause during periods of adverse climatic conditions (*5*). However, I believe that far too little consideration has been given to the possible undesirable effects on natural enemies, especially endoparasitoids. Two studies (*6*) of host-parasitoid complexes indicate that parasitoid development and fecundity are unaf-